Myosin complexed with ADP and blebbistatin reversibly adopts a conformation resembling the start point of the working stroke

Balázs Takács[a], Neil Billington[b], Máté Gyimesi[a], Bálint Kintses[a], András Málnási-Csizmadia[a], Peter J. Knight[b], and Mihály Kovács[a,1]

[a]Department of Biochemistry, Eötvös University, H-1117 Budapest, Pázmány Peter Setany 1/C, Hungary; and [b]Astbury Centre for Structural Molecular Biology and Institute of Molecular and Cellular Biology, University of Leeds, Leeds LS2 9JT, United Kingdom

The powerstroke of the myosin motor is the basis of cell division and bodily movement, but has eluded empirical description due to the short lifetime and low abundance of intermediates during force generation. To gain insight into this process, we used well-established single-tryptophan and pyrene fluorescent sensors and electron microscopy to characterize the structural and kinetic properties of myosin complexed with ADP and blebbistatin, a widely used inhibitor. We found that blebbistatin does not weaken the tight actin binding of myosin.ADP, but unexpectedly it induces lever priming, a process for which the gamma-phosphate of ATP (or its analog) had been thought necessary. The results indicate that a significant fraction of the myosin.ADP.blebbistatin complex populates a previously inaccessible conformation of myosin resembling the start of the powerstroke.

actomyosin | ATPase | kinetics | molecular motors | structure

Myosin produces force during cyclical interaction with actin and ATP. We and others have shown that blebbistatin, a potent and selective small-molecule inhibitor of myosin 2 (1), inhibits myosin ATPase and motile activity by blocking myosin (M) in a complex with ATP hydrolysis products (M.ADP.P$_i$) and slowing down phosphate (P$_i$) release (Fig. 1) (2, 3). This feature confers the great advantage that the inhibitor blocks myosin in a weak actin-binding state and, thus, the use of blebbistatin is not associated with adverse effects that could result from inhibitor-induced actin–myosin crosslinking within the cell. Blebbistatin (B) exerts its inhibitory effect by binding deep within the actin-binding cleft of the motor (catalytic) domain of myosin, between the nucleotide and actin-binding sites (Fig. 2) (3, 4). The atomic structure of the M.ADP.V$_i$.B complex [in which vanadate (V$_i$) is a P$_i$ analog] showed that the inhibitor causes only local conformational changes in this state, which is a well-characterized intermediate in the chemomechanical cycle of myosin (4). Myosin adopts this state after it detaches from actin in response to ATP binding, and hydrolyzes ATP while still detached from actin (Fig. 1). ATP hydrolysis is coupled to the priming of myosin's lever, and thus the M.ADP.P$_i$ posthydrolysis state is a weak actin-binding state with a prepowerstroke lever orientation (Fig. 1). In negative stain electron microscopy, the priming event is seen as a switch between a structure in which the lever is roughly colinear with the long axis of the motor domain to one in which there is a ∼90° bend between them (5). The primed state reassociates with actin (6), which process is coupled to activation of product release and a swing of myosin's lever that constitutes the powerstroke (Fig. 1). Although these events are crucial in the mechanism of force generation, the actin-bound powerstroke is the least-explored part of the working cycle in structural and mechanistic aspects (Fig. 1) (7).

In the present study, we assessed the effect of blebbistatin on the nucleotide-induced structural changes that occur during the working cycle of myosin. To this end, we utilized well-characterized single-tryptophan *Dictyostelium discoideum* myosin 2 (Ddm2) motor domain constructs that exhibit large and site-specific signal changes on different enzymatic steps (8–12). The W501+ construct contains a single native tryptophan in the relay-converter region, close to the base of the lever arm (Fig. 2). Kinking of the relay helix, coupled to closing of the switch-2 loop of the ATP binding site, leads to lever priming in the ATP-bound state (7, 13) and this is sensed by W501+ (12). The W239+ construct confers a sensor located in switch 1, another conserved loop of the ATP pocket (Fig. 2). Using this construct, earlier we showed that the closed–open motion of switch 1, which is a rapid step with an equilibrium constant close to unity, functions as a switch between low- and high-actin-affinity states (8).

Using the above single-tryptophan sensors here we show that, during the ATP hydrolysis cycle, blebbistatin stabilizes a closed switch-1 and closed switch-2 (weak actin-binding, prepowerstroke) myosin state, in line with earlier observations (2–4). However, we have come upon the striking conclusion that, in the absence of ATP and in the presence of ADP, blebbistatin induces a myosin structure with a closed switch 2 and a prepowerstroke lever orientation, which at the same time retains the switch-1 equilibrium distribution and high actin-binding affinity characteristic of the M.ADP complex. These features indicate that a significant fraction of the M.ADP.B complex populates a state resembling a functionally essential, "start-of-powerstroke" intermediate in the least-explored part of the force generation pathway. This intermediate has not been captured due to its low steady-state abundance and short lifetime in the absence of the inhibitor (Fig. 1) (7). Our findings on the blebbistatin-induced conformational changes in M.ADP are in line with previous x-ray diffraction results on muscle thick filaments and overstretched fibers showing helical ordering of myosin heads in similar conditions (14, 15).

Results

Blebbistatin Potently Inhibits Ddm2 Constructs. We investigated the effect of blebbistatin on the steady-state basal and actin-activated ATPase activities of the wild-type (M761) and single-tryptophan Ddm2 motor domain constructs used in this study (8, 12, 16). It was previously shown that Ddm2 is potently inhibited by blebbistatin (17, 18). Accordingly, we found similar blebbistatin inhibition profiles ($K_{1/2}$≈4 μM, maximal inhibition close to 100%) with all of our constructs (Fig. S1 and Table S1).

BIOCHEMISTRY

Fig. 1. Situation of the start-of-powerstroke state within the chemomechanical cycle of myosin. Binding of ATP to the actin-bound nucleotide-free (rigor) myosin motor domain (*Bottom Left*) causes cleft opening and actomyosin dissociation. Priming of the lever in an ATP-bound state (*Top Row*) is coupled to closing of the switch-2 loop of the ATP binding site. Following ATP hydrolysis (which occurs in the prepowerstroke state, *Top Right*), reassociation to actin is followed by the powerstroke and the coupled release of hydrolysis products. The start-of-powerstroke state (*Bottom Right, pink shade*), populated by ADP and blebbistatin, is the only principal state for which no atomic structure is available. [Note that, in the presence of ATP, blebbistatin stabilizes the well-characterized prepowerstroke state (*Top Right*), also shown in Fig. 2.]

Blebbistatin Induces Lever Priming in ADP. Using the well-characterized W501+ and W239+ single-tryptophan mutants (8–10, 12), we investigated the effect of blebbistatin on the nucleotide-induced fluorescence changes of myosin in the absence of actin. In the absence of blebbistatin, W501+ showed a small fluorescence quench on ADP addition, characteristic of a switch-2 open state, whereas ATP and ADP.AlF$_4^-$ (an ADP.P$_i$ analog) induced a large fluorescence increase, characteristic of the hydrolytically competent switch-2 closed state (Fig. 3*A*) (12). The open–closed transition of switch 2 has been shown to be associated with the priming of the lever whereby it moves from down (postpowerstroke) to up (prepowerstroke) orientation (9, 19). In blebbistatin, the ATP-induced fluorescence change was high and close to the ADP.AlF$_4^-$-induced one (Fig. 3*B*). This behavior is similar to
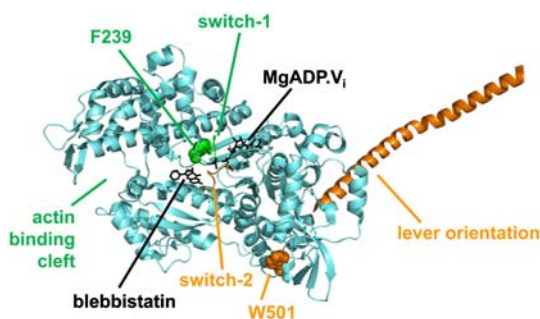
Fig. 2. Location of blebbistatin and single-tryptophan fluorescent sensors in the Ddm2 motor domain. Atomic structure of the Ddm2 catalytic domain complexed with MgADP.V$_i$ and blebbistatin (Protein Data Bank code: 1YV3) (4) is shown with the bound nucleotide and blebbistatin indicated as black stick representations. Structural elements whose conformation is sensed by W501 (switch 2 and the lever) and W239 (located in switch 1, proposed to be linked to the actin-binding cleft) are labeled and shown in orange and green, respectively. The structure contains F239, which is replaced by a tryptophan in the W239+ construct. The orange helix indicates the orientation of the lever, as inferred from aligning a scallop MgADP.V$_i$ S1 structure (1QVI) to 1YV3. Note that this is a closed switch-1 (weak actin binding) and closed switch-2 (primed lever) structure (prepowerstroke, *Top Right* in Fig. 1), different from the one proposed for M.ADP.B in the present study (start-of-powerstroke, *Bottom Right* in Fig. 1).

that in the absence of the inhibitor, indicating that the prepowerstroke M.ADP.P$_i$ state remains predominant during the ATPase cycle. Surprisingly, in ADP, blebbistatin induced a marked fluorescence increase, which extrapolated to the same W501+ fluorescence level as in ATP at high blebbistatin concentrations (the K_d of blebbistatin binding to M.ADP was 53 ± 16 μM; Fig. 3*C*). This behavior indicates that, in ADP, blebbistatin induces a switch-2 closed, primed-lever state. Such a structural state of myosin has never been observed in ADP; the presence of a ligand at the γ–P$_i$ binding site had been thought to be absolutely necessary for the priming of the lever. The closing of switch 2 in the M.ADP.B ternary complex is also indicated by the fact that the fluorescence increase was more pronounced at high temperatures, characteristic of the endothermic nature of the switch-2 open-closed transition (Fig. S2 *A* and *B*) (9). We further investigated the closure of switch 2 and the γ–P$_i$ pocket by assessing the effect of blebbistatin on the kinetics of formation of the myosin.ADP.AlF$_4^-$ complex (Fig. S3). Blebbistatin inhibited the kinetics of the formation of the complex precisely to the extent inferred from the fluorescence titration data (Fig. 3*C* and Fig. S3), which indicates that the M.ADP.B complex indeed has an inaccessible γ–P$_i$ binding pocket.

Kinetics of Formation of the M.ADP.B Complex. We could also measure the transient kinetics of formation of the M.ADP.B complex by monitoring W501+ fluorescence (Fig. S4). In line with the results shown in Fig. 3*C*, the data indicated that blebbistatin binds to M.ADP with medium affinity ($K_d = 42 \pm 10$ μM), which allows the formation of the ternary complex to significant levels (~70% of motor domains) near the solubility limit of blebbistatin (~100 μM).

Verification of Lever Priming by Electron Microscopy. Electron microscopy and single-particle image processing (20) was performed on rabbit skeletal myosin subfragment-1 (S1) rather than the Ddm2 motor domain, so that the orientation of the lever could be determined. This showed the expected colinear appearance of the motor domain and lever in apo and ADP-bound S1, and in contrast the bent structure of ADP-bound S1 with blebbistatin (Fig. 4*A*). Division of the data into more classes indicated that ~80% of molecules were in the bent conformation, consistent with the percentage of ternary complex formation in our conditions. The change in appearance closely resembles the difference between atomic structures thought to correspond to unprimed and primed S1, respectively (Fig. 4*B*). These results strongly indicate that the fluorescence changes in W501+ are indeed reporting lever movement, and that the M.ADP.B complex has a primed lever.

Actin Binding by the M.ADP.B Complex. We monitored the effect of blebbistatin on the nucleotide-induced conformational transitions of myosin also by using W239+, a construct containing a single tryptophan in the switch-1 loop. We have previously shown that the closing of this loop upon ATP binding (accompanied by a drop in W239+ fluorescence) is linked to a large reduction in actin affinity (possibly due to opening of the outer part of the actin-binding cleft), which results in ATP-induced dissociation of the myosin motor domain from the actin filament (8). In the present study, we found that the ATP-induced W239+ fluorescence drop was even higher in the presence of blebbistatin, whereas the ADP-induced fluorescence change was hardly affected by the inhibitor (Fig. 3 *D* and *E*). The W239+ fluorescence levels in ATP and ADP did not extrapolate to the same level at increasing blebbistatin concentrations, contrary to W501+ (Fig. 3 *C* and *F*). This behavior implies that blebbistatin does not markedly change the conformational equilibria of switch 1 and thus the actin-binding properties of myosin in different nucleotide states. Thus, whereas in ATP blebbistatin stabilizes
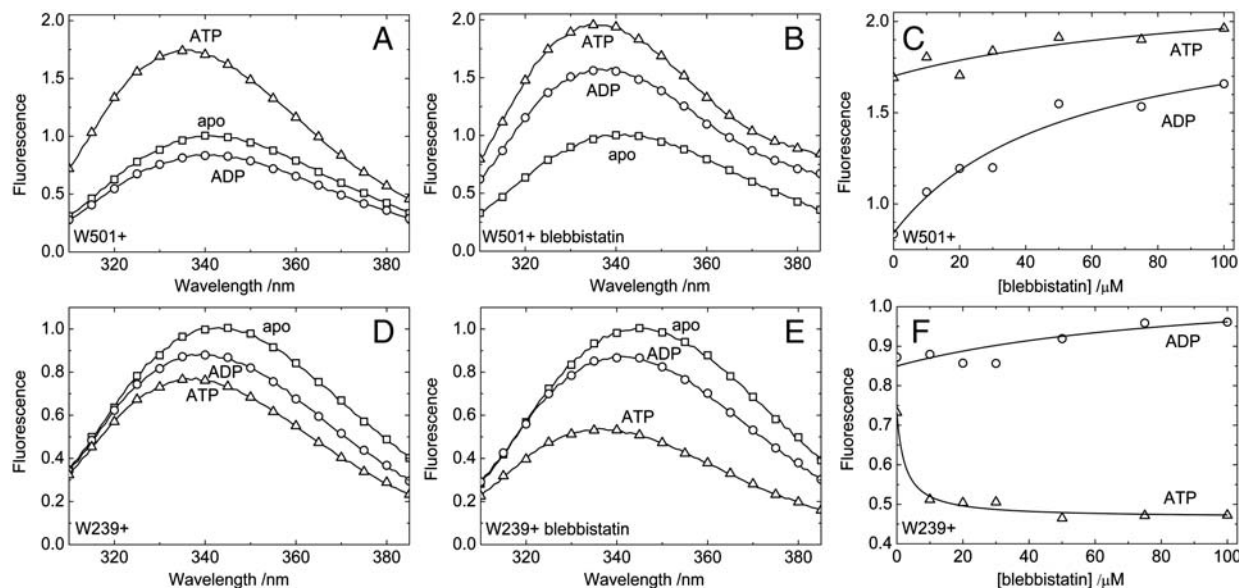
Fig. 3. Effect of blebbistatin on nucleotide-induced fluorescence changes of W501+ and W239+. (*A, B, D,* and *E*) Normalized tryptophan fluorescence emission spectra (excited at 297 nm) of W501+ (*A, B*) and W239+ (*D, E*) Ddm2 constructs (5 µM) in the absence (*A, D*) and in the presence (*B, E*) of blebbistatin (50 µM) in nucleotide-free state (□), in ADP (100 µM, ○) and in ATP (1 mM, △). In *C* (W501+) and *F* (W239+), normalized fluorescence intensities are plotted as a function of blebbistatin concentration in ADP (100 µM, ○) and in ATP (1 mM, △). In all cases, fluorescence intensities were normalized to the intensity maximum of the nucleotide-free state (one of three datasets is shown). Hyperbolic fits to the datasets of *C* and *F* were used to determine the extrapolated fluorescence levels at saturating blebbistatin concentrations, which were 2.2 ± 0.4 for W501+ in ADP, 2.1 ± 0.3 for W501+ in ATP, 1.1 ± 0.1 for W239+ in ADP, and 0.46 ± 0.04 W239+ in ATP. The curve for W501+ and ADP was also suitable for determining the blebbistatin binding K_d of W501 + .ADP as 53 ± 16 µM (cf. Fig. S4).
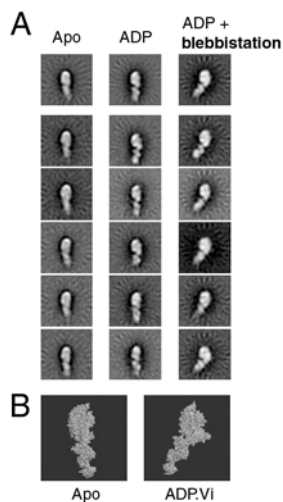
Fig. 4. Effect of ADP and blebbistatin on the structure of myosin S1. (*A*) Averaged images of rabbit skeletal myosin S1. Upper row shows global averages and below each panel the segregation of the images into five classes to explore variability in appearance. The motor domain is at the top of the images. *Left column*: apo-S1; *Center column*: S1 in the presence of 1 mM ADP; *Right column*: S1 in the presence of 1 mM ADP plus 100 µM blebbistatin. Panels are 31.2-nm wide. (*B*) Atomic structures of S1 oriented to resemble the typical motor domain appearance (*A*) in apo/ADP and ADP plus blebbistatin. *Left*: scallop apo S1 (1SR6); *Right*: scallop ADP.V$_i$ S1 (1QVI). Motor domains are oriented in the same direction for all panels in this figure. Note that this orientation is different from that shown in Fig. 2. Classification of S1 molecules in ADP and blebbistatin into a high number (30) of classes revealed the existence of two distinct conformations, one in which the lever is in the up position [82% of molecules, in agreement with the K_d of blebbistatin binding to M.ADP (Fig. S4)], and one with the lever in the down position. A small number of classes (5) is used to display all data in *A* so that the noise in images is reduced.

a weak actin-binding products complex with a closed switch 2, in ADP the ternary complex of myosin with ADP and blebbistatin retains high actin affinity (as in the absence of blebbistatin) due to the retained ability of switch 1 to open reversibly. To demonstrate that the presence of blebbistatin indeed does not change the actin-binding properties of myosin in different nucleotide states, we directly measured actin binding by ultracentrifugation-based actomyosin cosedimentation experiments. We found that the high actin affinity of both nucleotide-free and ADP-bound wild-type Ddm2 motor domain (K_d values close to 0.1 µM) was not significantly affected by blebbistatin (Fig. 5 *A* and *B*). Similarly, weak actin binding by the motor domain in the presence of ATP (K_d around 20 µM) was unaffected by blebbistatin (Fig. 5*C*).

We compared the actin (A) binding kinetics of M.ADP and M. ADP.B complexes in stopped-flow experiments monitoring tryptophan fluorescence and light-scattering changes upon actin binding by W239 + .ADP in the absence and presence of blebbistatin (Fig. S5 *A* and *B*). The process was associated with an 8% increase in total tryptophan fluorescence in all cases (absence and presence of blebbistatin Fig. S5*B Inset*). Considering that actin fluorescence constituted about 80% of the initial signal level at the applied concentrations, this increase is consistent with our earlier results whereby actin binding to W239 + .ADP induced a shift from a mixture of closed (low fluorescence) and open (high fluorescence) switch-1 states to a practically homogeneous open-switch-1 state, accompanied by a 36% increase in W239+ fluorescence (8). The concentration dependence of observed rate constants (k_{obs}) and amplitudes showed that both W239 + .ADP and W239 + .ADP.B form a strong-binding complex with actin ($K_d < 2$ µM, Fig. S5*B*).

This actin-binding behavior is very different from that of M.ADP.AlF$_4^-$, an analog of the M.ADP.P$_i$ posthydrolysis complex. In this state, W501+ exhibited a characteristic weak actin-binding profile whereby the rapid binding to actin (complete within less than 1 ms in light-scattering experiments) occurred at a K_d of 57 µM (6). To directly compare the actin-binding kinetics of W501 + .ADP.AlF$_4^-$ and W501 + .ADP.B complexes,
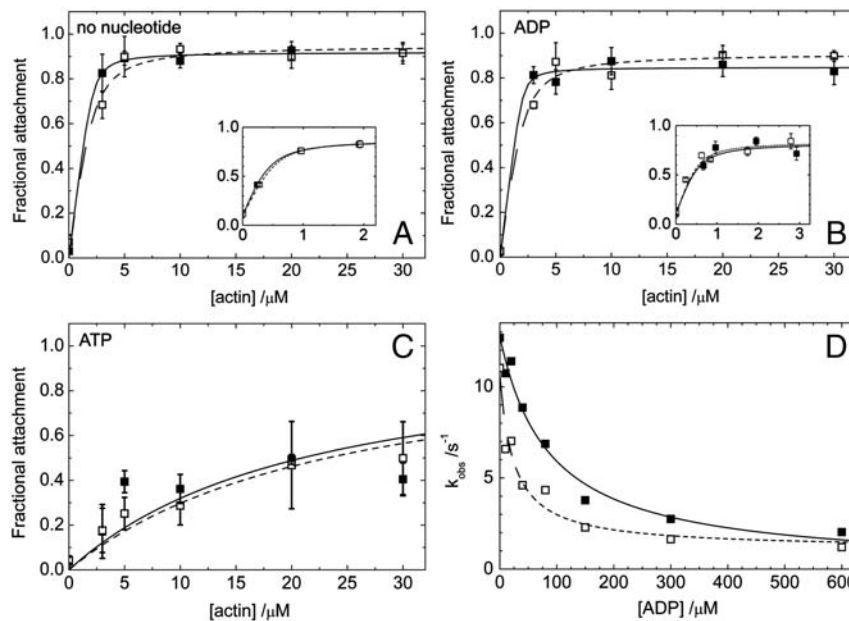
Fig. 5. Effect of blebbistatin on the actin-binding properties of wild-type Ddm2 catalytic domain and the ADP inhibition of ATP-induced actomyosin dissociation. The fractional attachment of the wild-type Ddm2 construct (M761, 2 μM) to F-actin filaments was determined by ultracentrifugation followed by SDS-PAGE densitometry. The fraction of actin-bound M761 in the nucleotide-free state (*A*), in ADP (100 μM, *B*) and in ATP (1 mM, *C*) is shown as a function of actin concentration in the absence (solid symbols) and in the presence of blebbistatin (100 μM, open symbols). Error bars indicate SD for $n = 4$. Quadratic fits to the data indicated actin-binding K_d values below 1 μM in no nucleotide and in ADP (both in the absence and presence of blebbistatin), and 20 ± 6 μM and 22 ± 3 μM in ATP in the absence and presence of blebbistatin, respectively. Insets in *A* and *B* show results obtained at 1 μM M761. Quadratic fits to the data resulted in actin-binding K_d values of 0.09 ± 0.04 μM (*A*, no blebbistatin), 0.11 ± 0.06 μM (*A*, 100 μM blebbistatin), 0.05 ± 0.04 μM (*B*, no blebbistatin), and 0.10 ± 0.06 μM (*B*, 100 μM blebbistatin). (*D*) ADP concentration dependence of the observed rate constant (k_{obs}) of ATP-induced actomyosin dissociation. The process was followed by measuring light-scattering changes in stopped-flow experiments upon rapidly mixing actomyosin (0.5 μM M761, 1 μM actin, plus the indicated ADP concentrations) with 200 μM ATP in the absence (solid symbols) and in the presence of blebbistatin (100 μM, open symbols). (Premixing concentrations are stated.) Hyperbolic fits to the data yielded a K_d for ADP binding to actomyosin of 69 ± 12 μM in the absence, and 24 ± 1 μM in the presence, of blebbistatin (one of two datasets is shown).

we performed stopped-flow experiments in which we monitored light-scattering changes upon actin binding by W501 + .ADP in the absence and presence of blebbistatin (Fig. S5 *C and D*). Similar to the W239+ data, the k_{obs} values and amplitudes indicated that W501 + .ADP.B binds strongly to actin, similar to W501 + .ADP (Fig. S5*D*). Taken together, the data of Fig. S5 showed that, although ADP-bound W239+ and W501+ exhibited different actin-binding kinetics, the M.ADP and M.ADP.B complexes had similar strong actin-binding characteristics in both constructs.

The above data suggest that, despite the fact that blebbistatin binds deep within myosin's actin-binding cleft, the M.ADP.B complex can bind to actin and form an A.M.ADP.B quaternary complex at high ADP and blebbistatin concentrations. We verified quaternary complex formation by two means. First, we investigated the effect of blebbistatin on the ADP inhibition of the ATP-induced dissociation of actomyosin (Fig. 5*D*). The data show that blebbistatin caused a 3-fold increase in the ADP affinity of actomyosin. Second, we measured the effect of increasing concentrations of blebbistatin on the fractional binding of M. ADP to actin in cosedimentation experiments (Fig. S6). In these experiments, the lack of a blebbistatin-induced reduction in the actin-bound fraction indicated that blebbistatin and actin can simultaneously bind to M.ADP.

AM.ADP.B Complex Significantly Populates a Strongly Actin-Bound State with a Primed Lever. The large nucleotide-induced fluorescence changes of the W501+ construct (Fig. 3 *A–C*) could be resolved even in the presence of actin and blebbistatin (Fig. 6*A*). Addition of ADP and ATP to acto-W501+ in the absence and presence of blebbistatin resulted in tryptophan fluorescence changes characteristic of actin-free W501+, indicating that the

presence of actin did not affect the overall distribution of lever orientations (Fig. 6*A*). These results indicate that ADP binding to acto-W501+ in the presence of blebbistatin induces a tryptophan fluorescence increase (reflecting lever priming) similar to that in the absence of actin (Fig. 3 *A–C*).

The K_d of blebbistatin binding to the AM.ADP complex (38 ± 17 μM; Fig. 6*A*) appeared to be very similar to that in M.ADP (37 μM, average from experiments of Fig. 3*C* and Fig. S4). The lack of coupling between actin and blebbistatin binding to M–ADP is consistent with the results of Fig. S6 and indicates that about 70% of the actin-bound motor domains populate the blebbistatin-bound (up-lever) state at high ADP (1 mM) and blebbistatin (100 μM) concentrations.

The identical W501+ fluorescence levels at saturating blebbistatin concentrations indicate that Ddm2 adopts the same lever orientation in all of the M.ADP.B, M.ADP.P$_i$.B, M.ADP.AlF$_4^-$.B, and AM.ADP.B states (Figs. 3*C* and 6*A*, and Fig. S2*B*). Interestingly, these blebbistatin-containing complexes showed significantly higher W501+ fluorescence levels than the well-characterized M.ADP.AlF$_4^-$.B up-lever complex (Fig. S2*A*). We attribute this difference to subtle differences in the conformational dynamics of the region involving W501+. In an earlier study, we found a similar effect caused by the K84M mutation at the base of the lever (21). Importantly, however, the M.ADP.V$_i$.B complex has been shown to adopt an up-lever conformation identical to those in blebbistatin-free up-lever states (4).

To monitor the distribution of strong and weak actin-binding Ddm2 states in the presence of nucleotides and/or blebbistatin, we monitored fluorescence changes of pyrene-labeled actin upon the addition of Ddm2 constructs (M761 and W501+) and ATP or ADP in the absence and presence of blebbistatin (Fig. 6*B* and
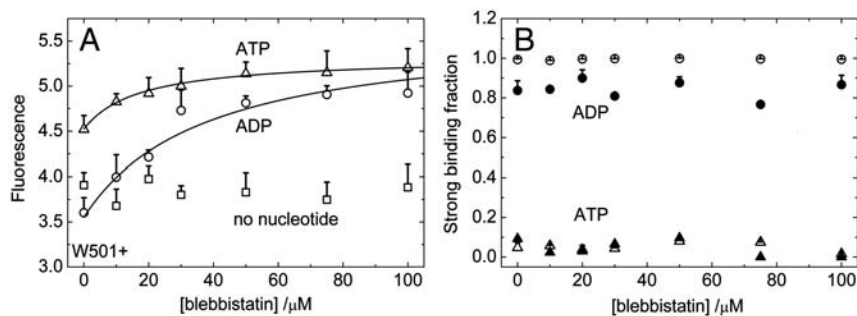
Fig. 6. Effect of blebbistatin on the fluorescent properties of acto–Ddm2 complexes. (*A*) Effect of blebbistatin on the tryptophan fluorescence intensity of 3 μM W501+ plus 5 μM actin in the absence of nucleotide (□), in ADP (500 μM, ○), and in ATP (1 mM, △). Fluorescence intensities were normalized to the intensity maximum of nucleotide-free W501+. Error bars represent the standard error for five sets of experiments. Hyperbolic fits to the datasets yielded blebbistatin binding K_d values of 38 ± 17 μM in ADP, and 17 ± 3 μM in ATP. The extrapolated W501+ fluorescence levels at saturating blebbistatin concentration were 2.6 ± 0.3 in ADP, and 2.4 ± 0.1 in ATP (with subtraction of actin fluorescence). (*B*) Fractional occupancy of myosin binding sites on pyrene-actin (PA) filaments by strongly bound M761 (solid symbols) and W501+ (open symbols) in the presence of ADP (circles), ATP (triangles), and blebbistatin. Values shown were determined based on pyrene fluorescence spectra of 3 μM PA alone, PA plus 5 μM Ddm2, PA plus Ddm2 plus 0.5 mM ADP, and PA plus Ddm2 plus 1 mM ATP, in the presence of different blebbistatin concentrations (Fig. S7), taking the peak fluorescence intensity of PA alone and PA plus Ddm2 (nucleotide-free) as zero and one, respectively (averages of two datasets are shown). Error bars represent the standard error for three sets of experiments.

Fig. S7). In these experiments, the binding of nucleotide-free and ADP-bound M761 to pyrene-actin resulted in fluorescence changes characteristic of the strong actomyosin interaction, regardless of the presence of blebbistatin (Fig. 6*B* and Fig. S7). These results, together with the tryptophan fluorescence experiments of Fig. 6*A* and the cosedimentation data of Fig. 5 *A* and *B*, strongly indicate that a significant proportion of actin-bound motor domains adopts an up-lever conformation in the presence of ADP and blebbistatin. The combined results of these experiments with those shown in Fig. 3*C* and Figs. S2–S4 exclude the possibility that any of the above conclusions drawn for the M.ADP.B complex could be affected by the presence of M.ADP.P$_i$.B heads remaining in the solutions after sample preparation.

Blebbistatin Binding to Apo-Myosin Does Not Induce Major Structural Changes. We also assessed the tryptophan fluorescence changes upon blebbistatin binding to the nucleotide-free (apo) Ddm2 motor domain. In these experiments, we used R(+) blebbistatin, the inactive enantiomer of the inhibitor (1), as a control to distinguish any tryptophan fluorescence changes induced by blebbistatin binding to Ddm2 from the significant inner filter effect arising from blebbistatin's light absorption. The data in Fig. S8 show that the binding of blebbistatin does not induce tryptophan fluorescence changes in W501+ and W239+ in the absence of nucleotide.

Discussion

Here we demonstrate that, upon binding ADP and blebbistatin, a significant fraction of myosin heads adopts an open-switch-1 state with a closed switch-2 loop and prepowerstroke (primed) lever orientation. This state went undetected in previous studies because it is not on the main pathway of the blebbistatin-inhibited myosin ATPase cycle. However, the properties of the M.ADP.B complex strongly indicate that one of its conformational states closely resembles a crucial yet unexplored intermediate of myosin's normal force generation cycle. The reassociation of the posthydrolytic M–ADP–P$_i$ complex to actin, and the subsequent events leading to product release and the powerstroke (force generation) form a crucial part of myosin's chemomechanical cycle, which is still unexplored after several decades of research (Fig. 1) (7). This set of events leads from a weak actin-binding (closed-switch-1) myosin state with a primed-lever arm and a closed switch 2 ("prepowerstroke" state in Fig. 1) to a tightly actin-bound (open-switch-1) state with a down lever arm ("rigor"; Fig. 1) (22, 23).

Based on a number of recent structural and spectroscopic studies, it is now considered highly unlikely that myosin's powerstroke would occur as a reversal of the structural changes triggered by ATP binding (the so-called recovery stroke) (7, 23). Instead, force generation is thought to proceed through an actin-bound start-of-powerstroke M.ADP.P$_i$ state in which the actin-binding cleft is already closed, but the lever is still in the up orientation (Fig. 1). Switch 2 stays closed throughout the subsequent swing of the lever to the down position, which constitutes the powerstroke. The release of the ATP hydrolysis products is facilitated via a conformational change of the P loop linked to the twisting of the central β-sheet of the motor domain (7). Thus it appears that a switch-2 closed, up-lever state in which switch 1 can open to allow high-affinity actin binding is an essential stage of the force generation pathway (6, 7). All of the results presented here suggest that the M.ADP.B complex characterized in this study is able to form this start-of-powerstroke state. Such a state is very difficult to characterize in the normal working cycle because of its very low abundance and short lifetime. Several atomic structures are now available for each of the three other principal myosin states, but structural knowledge of any start-of-powerstroke intermediate is lacking (Fig. 1). The solution data presented here also show that, in the presence of ADP and blebbistatin, the start-of-powerstroke state is in conformational equilibrium with the well-characterized prepowerstroke state, and thus crystallization conditions may affect the crystalline conformation of the ternary complex [as in earlier studies on the M.ADP.BeF$_x$ complex (13)]. Conformational heterogeneity resulting from internal equilibration and incomplete levels of saturation of myosin molecules with blebbistatin also poses technical difficulties in the electron microscopic visualization of the actoS1.ADP.B complex.

Helical ordering of ADP-bound (but not of nucleotide-free) myosin heads in tarantula thick filaments was recently observed in an x-ray diffraction and negative staining electron microscopic study by Zhao et al. (14). The ordered state of myosin heads was previously associated with the prepowerstroke state (24). In another x-ray diffraction study, Yu and coworkers also observed that, in overstretched muscle fibers, blebbistatin causes ordering of the myosin heads in the nonoverlapping (myosin-only) region (15). They detected significant blebbistatin-induced increases of the abundance of the ordered state in several different nucleotide states including ADP. Interestingly, we did not detect any effect of blebbistatin on the conformation of nucleotide-free myosin heads, contrary to the latter study (Fig. S8*A*) (15). Nevertheless, the above studies corroborate that blebbistatin induces the

prepowerstroke state regardless of the occupancy of the γ–P_i binding pocket. Importantly, however, none of the above works directly addressed the blebbistatin-induced lever priming, the active site conformation, or the actin-binding properties of the myosin.ADP.B complex.

We anticipate that further structural details of the myosin. ADP.B complex (and potentially its actin-bound form) identified in the present study will be of high utility in the understanding of the mechanism of force production by actomyosin. The coupling between switch 1 opening and cleft closure, and the possible capability of open-switch-1 states to bind to actin without significant conformational rearrangements, remain important issues to be addressed in future studies.

Methods

Materials. Wild-type (M761) and single-tryptophan (W501+ and W239+) Ddm2 constructs were expressed in *Dictyostelium* AX2–ORF+ cells and isolated using His-tag affinity chromatography as described previously (8, 12, 16). The purified motor domain constructs were dialyzed against an assay buffer containing 40 mM NaCl, 20 mM Hepes (pH 7.2), 2 mM MgCl$_2$, and 1 mM DTT. All experiments were performed in this buffer at 20 °C unless otherwise indicated. Actin was prepared as in ref. 25 and pyrene labeled as in ref. 26. Actin filaments were stabilized by addition of a 1.5-fold molar excess of phalloidin (Molecular Probes) in all experiments. Blebbistatin was purchased from Calbiochem. The active [S(-)] enantiomer of blebbistatin was used unless otherwise stated. Traces of ATP were carefully removed from ADP stock solutions by extensive preincubation with Ddm2 proteins. Rabbit skeletal papain-Mg S1 was prepared as described (27), and active molecules selected by a cycle of actoS1 cosedimentation, ATP release, and dialysis into 100 mM KCl, 10 mM MOPS, 0.1 mM EGTA, 2 mM MgCl$_2$ (pH 7.2), essentially as described (28).

Kinetic Measurements. Steady-state MgATPase activities were measured by an NADH-linked assay as described previously (29, 30) in 1 mM ATP. Data were corrected for background ATPase activity of actin. Stopped-flow experiments were carried out in a KinTek SF-2004 instrument. Tryptophan fluorescence was excited at 297 nm (2-nm bandwidth), and emission was detected using a 340-nm interference filter. Light scattering was measured at 320 nm. If not stated otherwise, postmixing concentrations are indicated throughout the text. Volume ratios in stopped-flow mixtures were 1:1 in all experiments.

Fluorescence Measurements. These experiments were carried out in a Spex320 FluoroMax spectrofluorometer equipped with a 150W Xe lamp, using a 10-mm path length cell. Tryptophan was excited at 297 nm using 4-nm excitation and emission slits. The temperature dependence of tryptophan fluorescence (detected at 345 nm) was measured by both cooling (from 22 to 4 °C) and reheating the samples. Pyrene fluorescence excitation and emission spectra were recorded at 406-nm emission and 365-nm excitation, respectively.

ActoS1 Cosedimentation. 100-μL samples were ultracentrifuged at 90,000 rpm in a Beckman TLA-100 rotor for 20 min at 4 °C, and the supernatants and pellets were analyzed by 4–20% SDS-PAGE. Relative amounts of proteins in electrophoretic bands were determined by densitometry using the Gene-Tools software (SynGene).

Electron Microscopy. Rabbit skeletal papain-Mg^{2+} S1 at 100 nM was either treated with 0.5 u/mL apyrase for 15 min to ensure it was in the apo state, or incubated in 1 mM ADP, 1 mM glucose, 0.5 u/mL hexokinase for 30 min at 20 °C. Blebbistatin was added to 100 μM and incubated 5 min. A drop of S1 was applied to a carbon-filmed EM grid and directly stained with 1% uranyl acetate. In micrographs, digitized at 0.52 nm/pixel, all S1-size particles were analyzed using SPIDER software as described (31), using reference-free alignment, a classification mask based on image variance, and K-means clustering.

Kinetics Data Analysis. Reported means and SD values are those of two to four rounds of experiment. Fits to the datasets were generated using the KinTek software and OriginLab 7.0 (Microcal).

1. Straight AF, et al. (2003) Dissecting temporal and spatial control of cytokinesis with a myosin II inhibitor. *Science* 299:1743–1747.
2. Ramamurthy B, Yengo CM, Straight AF, Mitchison TJ, Sweeney HL (2004) Kinetic mechanism of blebbistatin inhibition of nonmuscle myosin IIb. *Biochemistry* 43:14832–14839.
3. Kovacs M, Toth J, Hetenyi C, Malnasi-Csizmadia A, Sellers JR (2004) Mechanism of blebbistatin inhibition of myosin II. *J Biol Chem* 279:35557–35563.
4. Allingham JS, Smith R, Rayment I (2005) The structural basis of blebbistatin inhibition and specificity for myosin II. *Nat Struct Mol Biol* 12:378–379.
5. Burgess S, et al. (2002) The prepower stroke conformation of myosin V. *J Cell Biol* 159:983–991.
6. Gyimesi M, et al. (2008) The mechanism of the reverse recovery step, phosphate release, and actin activation of Dictyostelium myosin II. *J Biol Chem* 283:8153–8163.
7. Geeves MA, Holmes KC (2005) The molecular mechanism of muscle contraction. *Adv Protein Chem* 71:161–193.
8. Kintses B, et al. (2007) Reversible movement of switch 1 loop of myosin determines actin interaction. *EMBO J* 26:265–274.
9. Malnasi-Csizmadia A, et al. (2001) Kinetic resolution of a conformational transition and the ATP hydrolysis step using relaxation methods with a Dictyostelium myosin II mutant containing a single tryptophan residue. *Biochemistry* 40:12727–12737.
10. Malnasi-Csizmadia A, Kovacs M, Woolley RJ, Botchway SW, Bagshaw CR (2001) The dynamics of the relay loop tryptophan residue in the Dictyostelium myosin motor domain and the origin of spectroscopic signals. *J Biol Chem* 276:19483–19490.
11. Malnasi-Csizmadia A, Dickens JL, Zeng W, Bagshaw CR (2005) Switch movements and the myosin crossbridge stroke. *J Muscle Res Cell Motil* 26:31–37.
12. Malnasi-Csizmadia A, Woolley RJ, Bagshaw CR (2000) Resolution of conformational states of Dictyostelium myosin II motor domain using tryptophan (W501) mutants: Implications for the open-closed transition identified by crystallography. *Biochemistry* 39:16135–16146.
13. Geeves MA, Holmes KC (1999) Structural mechanism of muscle contraction. *Annu Rev Biochem* 68:687–728.
14. Zhao FQ, Padron R, Craig R (2008) Blebbistatin stabilizes the helical order of myosin filaments by promoting the switch 2 closed state. *Biophys J* 95:3322–3329.
15. Xu S, White HD, Offer GW, Yu LC (2009) Stabilization of helical order in the thick filaments by blebbistatin: further evidence of coexisting multiple conformations of myosin. *Biophys J* 96:3673–3681.
16. Kurzawa SE, Manstein DJ, Geeves MA (1997) Dictyostelium discoideum myosin II: Characterization of functional myosin motor fragments. *Biochemistry* 36:317–323.

17. Shu S, Liu X, Korn ED (2005) Blebbistatin and blebbistatin-inactivated myosin II inhibit myosin II-independent processes in Dictyostelium. *Proc Natl Acad Sci USA* 102:1472–1477.
18. Limouze J, Straight AF, Mitchison T, Sellers JR (2004) Specificity of blebbistatin, an inhibitor of myosin II. *J Muscle Res Cell Motil* 25:337–341.
19. Urbanke C, Wray J (2001) A fluorescence temperature-jump study of conformational transitions in myosin subfragment 1. *Biochem J* 358:165–173.
20. Burgess SA, Walker ML, Thirumurugan K, Trinick J, Knight PJ (2004) Use of negative stain and single-particle image processing to explore dynamic properties of flexible macromolecules. *J Struct Biol* 147:247–258.
21. Malnasi-Csizmadia A, et al. (2007) Selective perturbation of the myosin recovery stroke by point mutations at the base of the lever arm affects ATP hydrolysis and phosphate release. *J Biol Chem* 282:17658–17664.
22. Coureux PD, et al. (2003) A structural state of the myosin V motor without bound nucleotide. *Nature* 425:419–423.
23. Reubold TF, Eschenburg S, Becker A, Kull FJ, Manstein DJ (2003) A structural model for actin-induced nucleotide release in myosin. *Nat Struct Biol* 10:826–830.
24. Xu S, Offer G, Gu J, White HD, Yu LC (2003) Temperature and ligand dependence of conformation and helical order in Myosin filaments. *Biochemistry* 42:390–401.
25. Spudich JA, Watt S (1971) The regulation of rabbit skeletal muscle contraction. I. Biochemical studies of the interaction of the tropomyosin-troponin complex with actin and the proteolytic fragments of myosin. *J Biol Chem* 246:4866–4871.
26. Cooper JA, Walker SB, Pollard TD (1983) Pyrene actin: documentation of the validity of a sensitive assay for actin polymerization. *J Muscle Res Cell Motil* 4:253–262.
27. Margossian SS, Lowey S (1982) Preparation of myosin and its subfragments from rabbit skeletal muscle. *Methods Enzymol* 85(Pt B):55–71.
28. Yamashita H, Tyska MJ, Warshaw DM, Lowey S, Trybus KM (2000) Functional consequences of mutations in the smooth muscle myosin heavy chain at sites implicated in familial hypertrophic cardiomyopathy. *J Biol Chem* 275:28045–28052.
29. Trentham DR, Bardsley RG, Eccleston JF, Weeds AG (1972) Elementary processes of the magnesium ion-dependent adenosine triphosphatase activity of heavy meromyosin. A transient kinetic approach to the study of kinases and adenosine triphosphatases and a colorimetric inorganic phosphate assay in situ. *Biochem J* 126:635–644.
30. Wang F, et al. (2003) Kinetic mechanism of non-muscle myosin IIB: Functional adaptations for tension generation and maintenance. *J Biol Chem* 278:27439–27448.
31. Burgess SA, Walker ML, Sakakibara H, Oiwa K, Knight PJ (2004) The structure of dynein-c by negative stain electron microscopy. *J Struct Biol* 146:205–216.